



Double-pass wavefront shaping for scatter correction in a cataract's model

ALBA M. PANIAGUA-DÍAZ,^{1,*}  ALFONSO JIMÉNEZ-VILLAR,² 
IRENEUSZ GRULKOWSKI,²  AND PABLO ARTAL¹ 

¹Laboratorio de Óptica, Centro de Investigación en Óptica y Nanofísica (CiOyN), Universidad de Murcia, Campus de Espinardo (Ed. 34), 30100 Murcia, Spain

²Institute of Physics, Faculty of Physics, Astronomy and Informatics, Nicolaus Copernicus University, ul. Grudziądzka 5, 87–100 Toruń, Poland

*a.paniagua-diaz@um.es

Abstract: Cataracts are a common ocular pathology involving an increase in the amount of intraocular light scattering. This causes vision impairment by blurring and reducing the contrast in retinal images. The current treatment for this pathology is cataract surgery, which is an invasive procedure with possible side effects, such as corneal edema, infection or retinal detachment among others. In this work, we propose a non-invasive approach to improve vision through the cataractous lenses by manipulating the wavefront of the incident light. By using a fluorescent signal as feedback (similar to the inherent fluorescence of the lipofuscin pigment at the retina) we show the capability of improving the point spread function (PSF) of the eye in a single pass through the artificial eye's optics, while the feedback signal is measured in a double-pass configuration, making the whole system completely non-invasive, opening new possibilities for real-time vision correction through cataracts with wearable devices.

© 2021 Optical Society of America under the terms of the [OSA Open Access Publishing Agreement](#)

1. Introduction

The main problem arising with cataracts is the vision impairment, due to the blur and reduced contrast of retinal images [1]. Most cases of cataracts are related to the aging process, although there are children born with cataracts, or these can develop as a result of injuries, high exposure to UV light, or other eye diseases. Cataracts are responsible for over 51% of blindness in the Eastern Mediterranean Region (WHO 2021) if no action is undertaken, although this percentage is expected to grow as life expectancy increases. Currently the only solution to cataracts is surgery, where the eye's crystalline lens is removed and substituted by an artificial intraocular lens. Even though cataract surgery is a quick and easy intervention, apart from the potential side effects there are countries where access to eye care is restricted or patients who would strongly prefer a non-invasive solution if it only existed. In this work, we present an experiment where we manage to improve the Point Spread Function (PSF) of cataractous-like artificial eye in a non-invasive manner, paving the path for future real-time vision correction through cataracts.

A cataract is an opacification of the lens in the eye, caused by protein aggregation within the lens, scattering light in all directions, resulting in the blur and contrast loss of retinal images. Other than removing the scattering lens to avoid this effect (done in the cataract surgery), the other only option is trying to correct or control the scattering occurring inside the lens. Although the scattering process of light might appear completely random, the underlying physics is completely deterministic [2,3], which allows for some degree of control over it. Being able to control the propagation of light passing through scattering media is a challenge of interest in different fields and there is substantial effort put into overcoming this issue. In recent years wavefront shaping techniques appeared as an excellent tool to control the propagation of light through scattering materials, allowing focusing through such media [4], as well as being useful in other applications such as imaging [5–7], enhancing energy delivery [8–10] or cryptography [11,12], among others.

Wavefront shaping is based on the coherent control of the wavefront incident on a scattering medium using a Spatial Light Modulator (SLM), which allows the local manipulation of both phase and amplitude of the wavefront. In our case, we propose the use of wavefront shaping techniques to un-blur retinal images caused by the intraocular scattering. In general terms the image of an object can be described as the convolution of the imaging system's PSF and the real object, so the sharper the PSF is, the sharper the image. The imaging system of the eye is formed by the cornea and the ocular lens. When the lens develops cataracts, the eye's PSF (a sharp peak for young and healthy eyes [1]) flattens, resulting in a blurry vision. Given that the PSF of the eye is deteriorated by the scattering happening in the lens, it is possible to use wavefront shaping techniques to pre-compensate the scattering process, thus improving the PSF of the cataractous eye. When the wavefront leading to the optimal (or sharpest) PSF is added (as a phase or amplitude mask) to the imaging system, the image becomes sharper, consequently improving vision through cataracts. The use of wavefront shaping to improve the eye's PSF was recently proposed in our group, obtaining promising preliminary results when optimizing the eye's PSF through simulated nuclear cataracts of different clinical grades [13], although it was done in a single-pass through the scattering layer. The limitation of this approach is the fact that in order to provide a non-invasive solution, the wavefront needs to be optimized in a double-pass through the cataract, or in a reflection configuration. This poses an additional complexity to the approach, given that the incoming wavefront undergoes three different scattering processes, the incoming one, the retinal scattering mainly due to the structure of cones and rods, and the outgoing pass through the cataract. This implies that when analyzing the outgoing wavefront, if one tries to focus it to a diffraction limited spot, the outgoing pattern is not related to the pattern on the retina, which is the pattern of interest if one wants to optimize the eye's PSF to improve vision.

In order to avoid this problem, we use an approach similar to that used in [14] where the authors take advantage of the non-linearities to focus through scattering media in a non-invasive manner. We use a linear fluorescent signal as feedback that due to the different wavelength emission makes the ingoing and outgoing scattering processes independent from each other [2,3]. Thanks to the linearity of the process, when measuring the outgoing fluorescent intensity, it is possible to determine the shape of the incoming excitation wavefront to a certain degree, allowing in this manner to use the fluorescent intensity as feedback to shape the incoming wave in a completely non-invasive manner. In the case of the real eye, to make sure we are optimizing the beam at the retinal plane, we can use the natural fluorescence of the retina, the protein RPE lipofuscin. This protein absorbs light in the short wavelengths of the visible spectrum (blue - green) and emits in the red, around 600 nm [15]. As a first experimental demonstration of the idea, in this experiment we use an artificial eye with a diffusing and fluorescent layer working as the retina, with very similar emission and excitation spectra.

2. Experimental setup

A schematic of the experimental setup is shown in Fig. 1(a). A green laser (80 mW, EO PN 35072, Edmund Optics) with central wavelength of 532 nm is expanded and sent to a Spatial Light Modulator (SLM) to shape the wavefront in phase. We use a Digital Micromirror Device (DLP7000, Texas Instruments) for which the Lee Holography method is used in order to modulate the phase [16], that thanks to their high speeds (up to 22.7 kHz) could allow us to perform the experiment in real time. The shaped wavefront is then de-magnified by a factor 0.2x by the telescope formed by lenses L_1 and L_2 in a 4-f configuration. The size of the beam at the pupil plane (at the position of lens L_3) is 2.1×2.8 mm, similar to the typical pupil diameter size of 3 mm or smaller in elder people. This beam is then sent to an artificial cataractous eye, via a long-pass dichroic mirror (DM). The artificial eye consists of a lens L_3 , next to a silicon diffuser with a transport mean free path $\ell=4.45$ mm and a straylight parameter $\text{Log}_{10}(s) = 1.6$ at 3 degrees,

measured using with the Optical Integration Method [17] (equivalent to a moderate cataract) shown in Fig. 1(b). The thickness of the diffuser was chosen to be 3.5 mm, in order to match with the average thickness of a human crystalline lens. The diffuser is placed right behind lens L_3 , and a rough fluorescent layer (FL) acting as a diffusive retina, with the fluorescent spectra emission shown in Fig. 1(c) when excited with a wavelength of 532 nm. We used a piece of pink post-it as fluorescent layer.

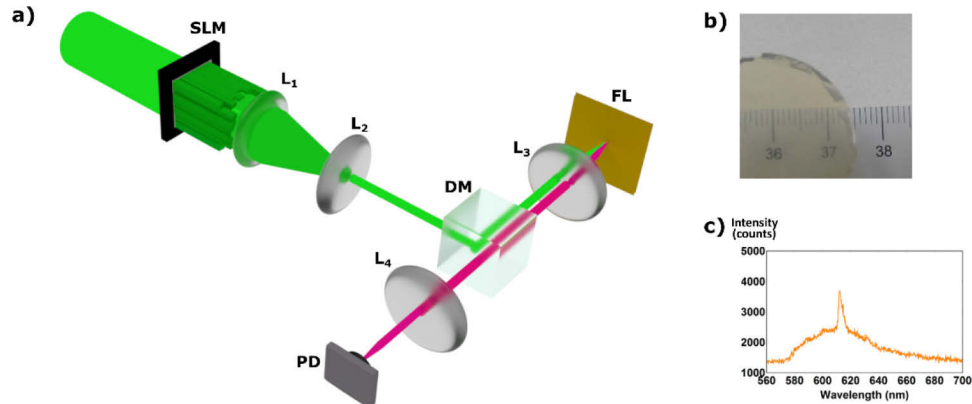


Fig. 1. (a) Schematic of the experimental setup. (b) Picture of one of the diffusers used as cataract phantom, with straylight parameter $\text{Log}_{10}(s) = 1.6$ at 3 degrees. (c) Spectral emission of the fluorescent layer used as artificial diffusive retina when excited with 532 nm.

The reflected fluorescence that exits the artificial eye is separated from the incident one with the long-pass dichroic mirror, which is then collected by a photodiode (PD), after passing through a $40\ \mu\text{m}$ pinhole that works as a spatial filter of diffraction limited size, in a conjugate retinal plane. The intensity collected by the photodiode works as feedback for an algorithm that controls the SLM, modifying the phase of the incident wavefront in order to increase the intensity reaching the photodiode at the filtered spot. A variation of the partitioning algorithm was used [18], which provides a compromise between the signal to noise ratio and speed of the process. The optimization loop in our case was of 5000 iterations. In this case the DMD was working with 64×85 phase elements, since the whole array (768×1024 pixels) was divided into macropixels of 12×12 mirrors each to allow the Lee Holography method.

3. Results

3.1. Point spread function optimization

To visualize better the beam profile, we had an experimental arrangement that allowed us to quickly swap the fluorescent layer (FL) with a CCD camera to rigorously examine the incident beam reaching the retinal plane. In the same way, we had another CCD to be swapped with the photodiode (PD) to properly see the returning fluorescent pattern, although for simplicity they are omitted in the schematic of Fig. 1(a).

In the experiments, the algorithm starts the optimization from an incident beam with a random profile, returning the fluorescent beam pattern shown in Fig. 2(a), consequence of the random incident beam pattern shown in Fig. 2(d), chosen in this way in order to start from the worst-case scenario. As the optimization evolves, and the fluorescence intensity filtered by the pinhole increases, the fluorescent pattern is forced to change, resulting in a sharper peak or focus, of the size of a diffraction limited spot, clearly visible in Fig. 2(b). Consequently, the incident beam changes the shape as well (Fig. 2(e)), becoming a much sharper function (or sharper PSF). A cross-section comparison of the improvement due to the optimization is shown in Fig. 2(c)

for the fluorescent light and in Fig. 2(f), for the incident beam. For the diffusers used and the experimental conditions described, we improved the Signal to Noise Ratio (SNR) of the optimized incident beam from approximately a value of 0 (in the case of the random initial beam as in Fig. 2(d)) to a value larger than 200 (as depicted in Fig. 2(f)), with a completely non-invasive approach.

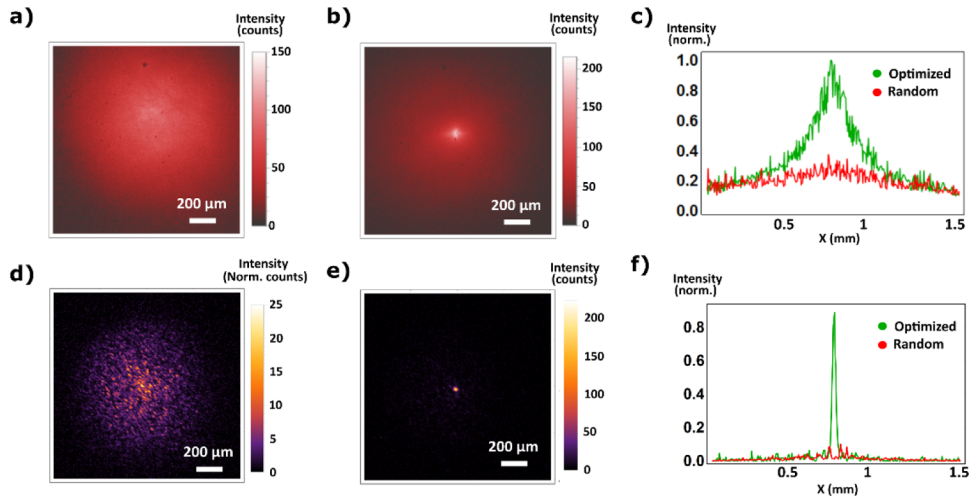


Fig. 2. Fluorescent beam pattern before (a) and after (b) the beam optimization. (c) Cross-section of the optimized and non-optimized fluorescent intensity patterns, corresponding to panels (a) and (b). (d) Incident beam pattern before (d) and after (e) the optimization. (f) Cross-section of the optimized and non-optimized incident intensity patterns.

However, this is not a realistic figure of merit, given that the incident beam was random by choice, not randomized to that extent by the diffuser itself. In Fig. 3(a) we plot the focal plane of an ideal beam that does not encounter any scattering event, the beam that undergoes the scattering at the diffuser (Fig. 3(b)) and the beam undergoing that same scattering after the wavefront correction (Fig. 3(c)). As it can be observed from the figure, the noise generated by the scattering is higher in panel (b) where the beam is not corrected, than for the corrected wavefront (panel (c)), and non-existent in the ideal case in panel (a). Using the ideal situation as reference for this comparison, we found out that when passing through the diffuser when no correction is implemented in the wavefront, the SNR reduces to 40% of the ideal one, whereas when the wavefront has been corrected, the SNR increases between 70 to 80%, in the particular case of the shown measurement in Fig. 3(c) the SNR is 75% with respect to the ideal case.

3.2. Image formation simulation

In order to gain intuition on what the improvement in the SNR means in terms of visual quality, we performed a simple image formation simulation. In simple terms, the image of an object is given by the convolution of the object itself and the PSF of the imaging system:

$$I(x,y) = O(x,y) * PSF(x,y) \quad (1)$$

Based on this equation, we simulated the image reconstruction with the different PSFs. In Fig. 3 we present the experimentally measured PSFs of the incident beam at the retinal plane, in the case of an ideal PSF, the deteriorated PSF after passing through the diffuser and the PSF of the optimized wavefront passing through the diffuser, simulating the situation of corrected vision through cataracts.

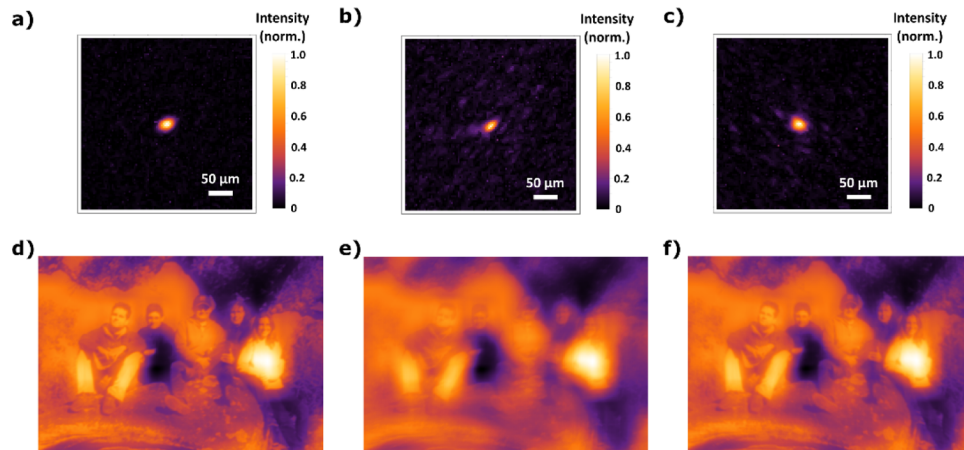


Fig. 3. (a) PSF of a Gaussian beam at the retinal plane. (b) PSF of a Gaussian beam passing through a diffuser with $\text{Log}_{10}(s) = 1.6$ at 3 degrees. (c) PSF of the optimized beam passing through the diffuser at the retinal plane. (d) Image of a picture convolved with the PSF of panel (a). (e) Image of a picture convolved with the PSF of panel (b). (f) Image of a picture convolved with the PSF of panel (c).

Assuming isoplanatism [19,20], that is, a situation in which the optimized PSF remains unchanged along the full extension of the image, we can do a quick simulation of the quality of the resulting images allowed by the previous PSFs, that can be seen in Fig. 3(d)-(f), respectively. As we can observe from the images, the uncorrected PSF of the diffuser blurs considerably the image, to the point in which the faces are difficult to even recognize. However, this effect can be undone or considerably improved by shaping the wavefront that is incident on the diffuser, in a completely non-invasive manner, retrieving image qualities comparable to the case where no diffuser is present (Fig. 3(d)).

4. Discussion and conclusions

We have demonstrated the capabilities of using wavefront shaping techniques for improving the PSF through the cataractous lens model. Even though the experiment presented here is done with an artificial eye, which allows us to optimize all the parameters in the system, the goal is to do it in real-time. The system has been built so that it is scalable to use it in vivo, doing the optimizations in real-time, thanks to the switch rates of the DMD, finishing the optimization in less than a second, when the DMD's FPGA is programmed. This will prevent rapid eye movement to disturb the optimization. The optimization process is designed to be robust even if rapid eye movement appear. Pupil positioning will be monitored in real time and it can pause the optimization in the cases where saccades or microsaccades are detected. Since the optimal wavefront depends on the scattering distribution, it is very important that the medium (the cataractous lens in this case) remains still during the measurement and later on. A factor that helps in this case is the fact that with age and presbyopia the lens loses its accommodation capability, so the scattering distribution remains the same in the short term. Long term changes (in the order of a few months) as the cataract develops can be accounted for, by re-measuring the wavefront when the correction loses quality.

For the image formation quality assessment, we have assumed isoplanatism for a quick simulation on image formation. This assumption is taken for simplicity, although there will always be a region where this assumption is true, the so-called isoplanatic patch. The size of this patch will be mainly determined by the scattering properties of the scattering medium (the

cataract in this case), as well as the thickness of it [21]. However, in the case the isoplanatic patch is too small as to form a regular image, the use of rapid tilting devices such as galvo mirrors could be considered, to project the corrected image in a mosaic-like approach, with different wavefront correction for the different angles, all of this at a high frequency, so that the eye perceives a single smooth and corrected picture. However, this approach might not be necessary, it is currently under study.

When moving to a real eye and a realistic situation, there will be also other challenges regarding chromaticity. Each wavefront correction is only valid for a given wavelength with a small linewidth, so when aiming at correcting a real image, the correction for red, green and blue should be sequentially displayed, multiplexed in time, so that to achieve a realistic image reconstruction in terms of color. In terms of the final wearable device for the correction, it will be based on active glasses, powered by spatial light modulators technology, that will display the correction in phase at the pupil plane.

In conclusion, we have demonstrated the possibility to improve the PSF of a moderate cataract phantom in a double-pass configuration using wavefront shaping techniques, together with the retinal-like fluorescence as feedback. We showed an almost two-fold increase in the SNR ratio of the optimized PSF with respect to the uncorrected one. In the imaging process simulation, we showed how the optimized PSF unblurs considerably the image, resulting very similar to that of the ideal PSF when no cataracts or diffusers are present. This approach opens new possibilities to the real-time correction of vision through cataracts in a non-invasive manner by wearable devices, paving the path for a potential alternative to surgery.

Funding. Agencia Estatal de Investigación (PID2019-105684RB-I00/AEI/10.13039/501100011033); Fundación Séneca (19897/GERM/15); Horizon 2020 Framework Programme (897300, Marie Skłodowska Curie Individual Fellowship); Fundacja na rzecz Nauki Polskiej (POIR.04.04.00-00-5C9B/17-00); Narodowa Agencja Wymiany Akademickiej (PPN/IWA/2019/1/00208/ROZ/00001); Narodowe Centrum Nauki (2017/26/M/NZ5/00849).

Acknowledgments. We thank Mr. Adrián Gambín Regadera for his support on the software development and Dr. Jacopo Bertolotti for discussions.

Disclosures. The authors declare that there are no conflicts of interest.

Data availability. The data underlying the results presented in this paper are available in Ref. [22].

References

1. P. Artal, *Handbook of Visual Optics, Two-Volume Set*. (CRC Press, 2017).
2. E. Akkermans and G. Montambaux, *Mesoscopic physics of electrons and photons* (Cambridge University, 2007)
3. J.W. Goodman, *Speckle phenomena in optics: theory and applications* (Roberts and Company Publishers, 2007)
4. I. M. Vellekoop and A. P. Mosk, "Focusing coherent light through opaque strongly scattering media," *Opt. Lett.* **32**(16), 2309–2311 (2007).
5. I. N. Papadopoulos, S. Farahi, C. Moser, and D. Psaltis, "High-resolution, lensless endoscope based on digital scanning through a multimode optical fiber," *Biomed. Opt. Express* **4**(2), 260–270 (2013).
6. T. Čižmár and K. Dholakia, "Exploiting multimode waveguides for pure fibre-based imaging," *Nat. Commun.* **3**(1), 1027 (2012).
7. E. G. van Putten, D. Akbulut, J. Bertolotti, W. L. Vos, A. Lagendijk, and A. P. Mosk, "Scattering lens resolves sub-100 nm structures with visible light," *Phys. Rev. Lett.* **106**(19), 193905 (2011).
8. A. M. Paniagua-Diaz, A. Ghita, T. Vettenburg, N. Stone, and J. Bertolotti, "Enhanced deep detection of Raman scattered light by wavefront shaping," *Opt. Express* **26**(26), 33565–33574 (2018).
9. O. S. Ojambati, H. Yılmaz, A. Lagendijk, A. P. Mosk, and W. L. Vos, "Coupling of energy into the fundamental diffusion mode of a complex nanophotonic medium," *New J. Phys.* **18**(4), 043032 (2016).
10. W. Choi, M. Kim, D. Kim, C. Yoon, C. Fang-Yen, Q. H. Park, and W. Choi, "Preferential coupling of an incident wave to reflection eigenchannels of disordered media," *Sci. Rep.* **5**(1), 11393 (2015).
11. R. Horstmeyer, B. Judkevitz, I. M. Vellekoop, and C. Yang, "Secure storage of cryptographic keys within random volumetric materials," in: *Conference on Lasers & Electro-Optics (CLEO): Applications and Technology* (2013), pp. AF1H-6.
12. S. A. Goorden, M. Horstmann, A. P. Mosk, B. Škorić, and P. W. Pinkse, "Quantum-secure authentication of a physical unclonable key," *Optica* **1**(6), 421–424 (2014).
13. A. Arias and P. Artal, "Wavefront-shaping-based correction of optically simulated cataracts," *Optica* **7**(1), 22–27 (2020).

14. O. Katz, E. Small, Y. Guan, and Y. Silberberg, "Noninvasive nonlinear focusing and imaging through strongly scattering turbid layers," *Optica* **1**(3), 170–174 (2014).
15. J. R. Sparrow and T. Duncker, "Fundus autofluorescence and RPE lipofuscin in age-related macular degeneration," *J. Clin. Med.* **3**(4), 1302–1321 (2014).
16. W. H. Lee, "Binary computer-generated holograms," *Appl. Opt.* **18**(21), 3661–3669 (1979).
17. H. S. Ginis, G. M. Pérez, J. M. Bueno, and P. Artal, "The wide-angle point spread function of the human eye reconstructed by a new optical method," *J. Vis.* **12**(3), 20 (2012).
18. I. M. Vellekoop and A. P. Mosk, "Phase control algorithms for focusing light through turbid media," *Opt. Commun.* **281**(11), 3071–3080 (2008).
19. D. L. Fried, "Anisoplanatism in adaptive optics," *J. Opt. Soc. Am.* **72**(1), 52 (1982).
20. R. Horstmeyer, H. Ruan, and C. Yang, "Guidestar-assisted wavefront-shaping methods for focusing light into biological tissue," *Nat. Photonics* **9**(9), 563–571 (2015).
21. S. Schott, J. Bertolotti, J. F. L  ger, L. Bourdieu, and S. Gigan, "Characterization of the angular memory effect of scattered light in biological tissues," *Opt. Express* **23**(10), 13505–13516 (2015).
22. A. M. Paniagua-D  az, A. Jim  nez-Villar, I. Grulkowski, and P. Artal, "Dataset for "Double-pass wavefront shaping for scatter correction in a cataract's model"," Zenodo (2021), <https://doi.org/10.5281/zenodo.5723978>.